Multinuclear Palladium Olefin Polymerization Catalysts Based On Self-Assembled Zinc Phosphonate Cages

Qian Liu and Richard F. Jordan*

Department of Chemistry, The University of Chicago, 5735 South Ellis Avenue, Chicago, Illinois 60637, United States

ABSTRACT: The phosphine-phosphonate-sulfonate proligand HP^+(4-^{t}Bu-Ph)(2-PO_3H_2-5-Me-Ph)(2-SO_3^--5-Me-Ph) (H_3[OP-P-SO], **1**-H_3) was investigated as a building block for the self-assembly of multinuclear Pd compounds based on zinc phosphonate scaffolds. **1**-H_3 reacts with $Zn(OAc)_2$•$2H_2O$ to afford {Zn[**1**-H]}$_4$, which adopts a $Zn_4P_4O_8$ ring structure in which the Zn centers are linked by μ^2-κ^1,κ^1-bridging (aryl)PO_3H^- ligands. {Zn[**1**-H]}$_4$ reacts with (TMEDA)$PdMe_2$ and pyridine to generate {[(κ^2-*O*P-*P*-SO)PdMe(py)][Zn(TMEDA)]}$_2$ (**2**), in which two [(κ^2-*O*P-*P*-SO)PdMe(py)]$^{2-}$ units are linked through a $Zn_2P_2O_4$ ring. The sequential reaction of CH_3OH-free {Zn[**1**-H]}$_4$ with (COD)$PdMe_2$ and 4-^{t}Bu-py generates {[κ^2-(Zn-OP-*P*-S*O*)]PdMe(4-^{t}Bu-py)}$_4$ (**4**-(4-^{t}Bu-py)), in which four [(κ^2-OP-*P*-S*O*)PdMe(4-^{t}Bu-py)]$^{2-}$ units are arranged on the periphery of a double-four-ring (D4R) $Zn_4P_4O_{12}$ cage. Analogous **4**-L species were generated by the reaction of {Zn[**1**-H]}$_4$, (COD)$PdMe_2$ and other pyridine ligands. **4**-py reacts with CH_3OH to form a trimeric cluster **3**-py, which adopts a cage structure based on $Zn_3P_3O_6$ and Pd_3O_3 rings. In the presence of $B(C_6F_5)_3$ to sequester the pyridine ligands, **4**-(4-^{t}Bu-py) and **3**-py polymerize ethylene at 80 ˚C to linear polyethylene with high molecular weight (up to M_w = ca. 1 x 10^6 Da).

INTRODUCTION

The phosphine-bis(arenesulfonate) palladium complex (Li-OPO)PdMe(py') (**A**, Scheme 1; LiOPO$^-$ = PPh(2-SO_3Li-5-Me-Ph)(2-SO_3^--5-Me-Ph), py' = 4-(5-nonyl)-pyridine) self-assembles into a tetrameric structure $\mathbf{A_4}$, in which four (Li-OPO)PdMe(py') units are arranged on the periphery of a double-four-ring (D4R) cage formed by the non-Pd-bonded Ar-SO_3Li groups.[1] $\mathbf{A_4}$ undergoes partial and reversible dissociation into monomeric **A** in solution. $\mathbf{A_4}$ polymerizes ethylene to linear polyethylene (PE) and copolymerizes ethylene with vinyl fluoride. The polymerization behavior of $\mathbf{A_4}$ is strongly influenced by the extent of disassembly under polymerization conditions. Under conditions where $\mathbf{A_4}$ is partially dissociated (hexanes slurry at 80 °C or CH_2Cl_2 solution at 25 °C), linear PE with a broad bimodal molecular weight distribution (MWD) comprising high-MW (ca. 10^6 Da) and low-MW (ca. 10^4 Da) fractions is produced. Under conditions where $\mathbf{A_4}$ is fully dissociated (dilute toluene solution at 80 °C), linear PE with a low MW (ca. 10^4 Da) and a Schulz-Flory MWD typical of mononuclear (phosphine-arenesulfonate)PdR catalysts is produced.[2] These results suggest that intact Pd_4 species produce the high MW fraction, while Pd_1 species produce the low MW fraction.

A current goal in this area is to design analogues of $\mathbf{A_4}$ that are more robust under polymerization conditions, to enable mechanistic studies to probe why intact $\mathbf{A_4}$ produces high-MW PE and make possible new applications in copolymerization.[3] One strategy for enhancing the stability of the central cage in Pd_4 assemblies such as $\mathbf{A_4}$ is to replace the Li^+ cations and sulfonate anions with stronger Lewis acid/base pairs. This paper explores the synthesis of analogues of $\mathbf{A_4}$ that are based on Zn phosphonate cages.[4]

Scheme 1. Self-assembly and structure of {(Li-OPO)PdMe(py')}$_4$ ($\mathbf{A_4}$, py' = 4-(5-nonyl)-pyridine). The lower (Li-OPO)PdMe(py') units in the schematic structure of $\mathbf{A_4}$ are denoted by "Pd".

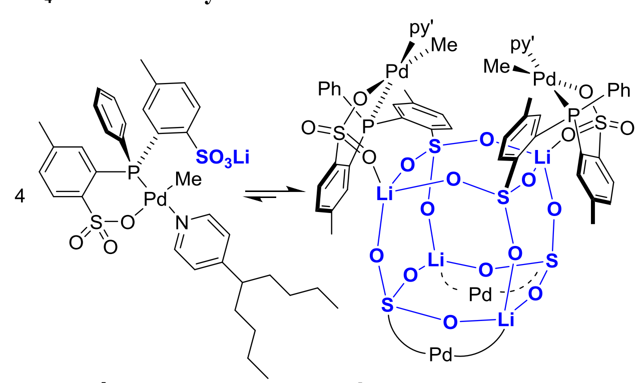

A $\mathbf{A_4}$, py' = 4-(5-nonyl)-pyridine

Molecular zinc phosphonate clusters exhibit a diverse range of structures and phosphonate coordination modes (Chart 1).[5] Dimeric zinc phosphonate compounds typically contain $Zn_2P_2O_4$ rings with doubly-bridging phosphonate groups (2.110 bonding mode in the Harris notation),[6,7] as exemplified by Zn_2{(3,5-^{t}Bu_2-2-OH-Ph)CH_2PO_3}$_2$(TMEDA)$_2$(H_2O)$_2$ (**B**).[6d] The trinuclear compound Zn_3Cl_2(3,5-Me_2-PzH)$_4$(^{t}BuPO_3)$_2$, (**C**, PzH = pyrazole) contains an interesting core structure in which the three zinc centers are linked by two triply-bridging (3.111) ^{t}BuPO_3^{2-} ligands.[8] The tetranuclear compound [Zn_4(2,4,6-^{i}Pr_3-Ph-PO_3)$_2${2,4,6-^{i}Pr_3-Ph-PO_3H}$_2$(3,5-Me_2-PzH)$_4$(3,5-Me_2-Pz)$_2$] (**D**) adopts a 2-dimensional tricyclic structure,[9] while [Zn_4(FMPA)$_4$(phen)$_4$] (**E**, FMPA = (ferrocenyl)$CH_2PO_3^{2-}$, phen = 1,10-phenanthroline) adopts a 3-

Chart 1. Representative structures of molecular Zn phosphonates. The lower (phosphine-sulfonate)PdMe(L) units in G are denoted by "Pd".

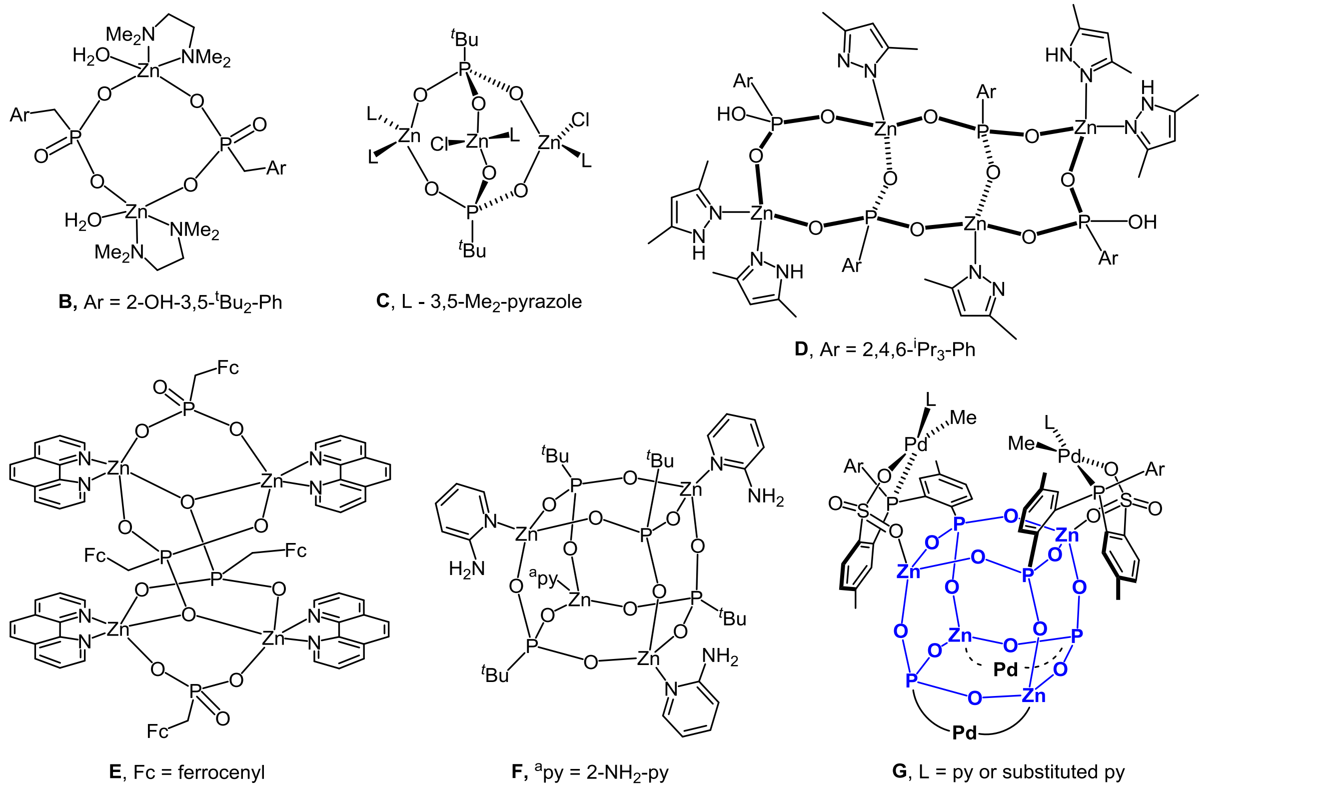

dimensional cage structure with two 2.110 and two 4.211 bridging phosphonates.[10]

[^{t}BuPO$_3$Zn(2-apy)]$_4$ (**F**, 2-apy = 2-amino-pyridine, Chart 1) was the first zinc phosphonate compound reported to contain a D4R cage structure.[11,12] Murugavel and coworkers synthesized **F** by the reaction of ^{t}BuPO$_3$H$_2$ and Zn(OAc)$_2$ with 2-apy to cap the Zn corners. The NH$_2$ group of the 2-apy ligand engages in intermolecular H-bonding which links the [^{t}BuPO$_3$Zn(2-apy)]$_4$ cages into a 3-dimensional polymer. The metrical parameters for the core cage of **F** are similar to those of the Li$_4$S$_4$O$_{12}$ cage in **A$_4$**. TGA analysis of **F** shows that the first weight loss occurs at 170–200 ˚C and is due to the loss of 2-apy, suggesting that the Zn$_4$P$_4$O$_{12}$ core is thermally robust.[13]

Based on Muragavel's studies of **F**, we envisioned that a (phosphine-arenesulfonate)PdMeL species containing a pendant Zn phosphonate group would adopt an analogous D4R cage structure **G** (Chart 1) that would be more thermally robust that **A$_4$**. Here we report the synthesis of a phosphine-phosphonate-sulfonate ligand, [P(4-^{t}Bu-Ph)(2-PO$_3$-5-Me-Ph)(2-SO$_3$-5-Me-Ph)]$^{3-}$ ([OP-P-SO]$^{3-}$) and its use as a scaffold for Zn$_4$, Zn$_2$Pd$_2$, Zn$_3$Pd$_3$ and Zn$_4$Pd$_4$ assemblies, the latter of which adopts the target structure **G**. The ethylene polymerization behavior of the Zn$_3$Pd$_3$ and Zn$_4$Pd$_4$ compounds is also reported.

RESULTS AND DISCUSSION

Synthesis of phosphine-phosphonate-sulfonate proligand HP$^+$(4-^{t}Bu-Ph)(2-PO$_3$H$_2$-5-Me-Ph)(2-SO$_3^-$-5-Me-Ph) (H$_3$[OP-P-SO], 1-H$_3$). Proligand **1**-H$_3$ was synthesized as shown in Scheme 2. The reaction of (4-^{t}Bu-Ph)PCl$_2$ with 2 equiv of HNEt$_2$ gave mono-protected (4-^{t}Bu-Ph)P(NEt$_2$)Cl. Reaction of this compound with *ortho*-lithiated diethyl *p*-toluenephosphonate and removal of the NEt$_2$ protecting group with HCl afforded (4-^{t}Bu-Ph)(2-PO$_3$Et$_2$-5-Me-Ph)PCl. The reaction of this intermediate with Li[*p*-toluenesulfonate] generated Li[**1**-Et$_2$] in 79 % ^{31}P NMR yield. Li[**1**-Et$_2$] was acidified with HCl to form H[**1**-Et$_2$] in 98 % yield. The reaction of H[**1**-Et$_2$] with SiMe$_3$Br followed by quenching with CH$_3$OH afforded **1**-H$_3$ in 78 % yield.

Synthesis of {Zn[H(OP-P-SO)]}$_4$ ({Zn[1-H]}$_4$). Following Murugavel's strategy for the synthesis of Zn phosphonate cage compound **F**, we envisioned that the reaction of **1**-H$_3$ with Zn(OAc)$_2$•2H$_2$O would afford D4R cage structure **H** with the sulfonate group capping the Zn centers (Scheme 3), which subsequently could be metalated to form target **G.** However, when conducted in CH$_3$OH with a small amount of CH$_2$Cl$_2$ to dissolve **1**-H$_3$, this reaction instead produces a 2-dimensional Zn phosphonate product, {Zn[**1**-H]}$_4$. {Zn[**1**-H]}$_4$ can be isolated by filtration and contains variable amounts of CH$_3$OH (2 to 64 equiv per {Zn[**1**-H]}$_4$ unit by NMR). The CH$_3$OH can be completely removed by heating under vacuum (50 °C, 2d).

Crystallization of {Zn[**1**-H]}$_4$ from CH$_3$OH solution (ca. 0.02 M in Zn^{2+}) affords X-ray quality crystals of {Zn[**1**-H](CH$_3$OH)}$_4$•12CH$_3$OH, the solid-state structure of which is shown in Figure 1.[14] The structure of {Zn[**1**-H](CH$_3$OH)}$_4$ features a puckered 16-membered Zn$_4$P$_4$O$_8$ ring in which the Zn centers are linked by μ^2-κ^1,κ^1 (aryl)PO$_3$H$^-$ bridges similar to those in **D**.[6d] {Zn[**1**-H](CH$_3$OH)}$_4$ has C_i symmetry with *SSRR* configurations at the phosphine P atoms. The Zn^{2+}-coordinated CH$_3$OH molecules form intramolecular H-bonds with the ArSO$_3^-$ or ArPO$_3$H$^-$ groups. Twelve additional CH$_3$OH molecules are present in the voids between the {Zn[**1**-H](CH$_3$OH)}$_4$ {Zn[**1**-H](CH$_3$OH)}$_4$ molecules and form an extensive H-bonding network.

Scheme 2. Synthesis of H_3[OP-P-SO] (1-H_3).

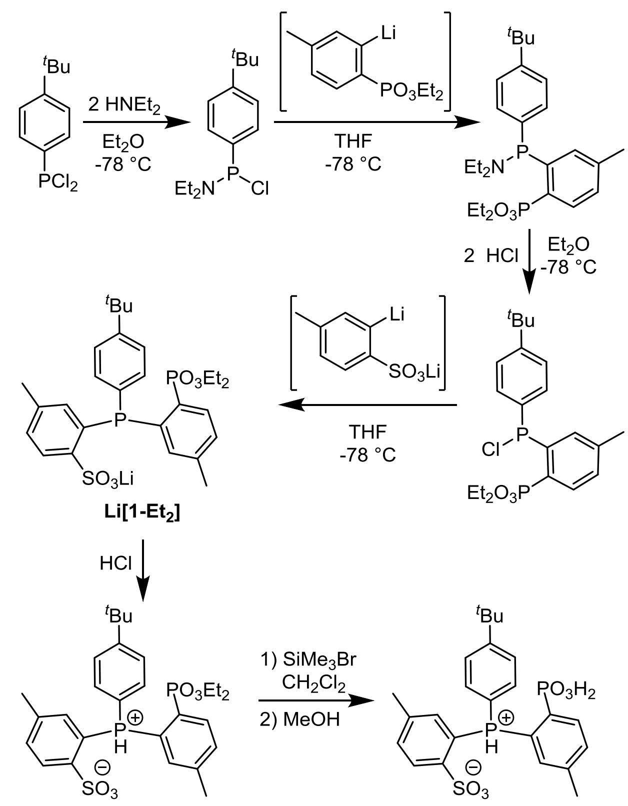

Solution Behavior of {Zn[1-H]}$_4$. The ^{31}P{^{1}H} NMR spectrum of {Zn[**1**-H]}$_4$•nCH$_3$OH (n = 0 to 64) in dmso-d_6 contains one phosphine resonance (δ -17.6) and one phosphonate resonance (δ 12.1, broad). The ^{1}H NMR spectrum of {Zn[**1**-H]}$_4$ is broad, but contains only one set of resonances, consistent with a highly symmetric structure in solution. The CH_3OH resonance appears at the chemical shift of free CH_3OH in dmso-d_6 (δ 3.17),[15] indicating that the CH_3OH is labile. The hydrodynamic volume of {Zn[**1**-H]}$_4$ determined by pulse-gradient-spin-echo (PGSE) NMR in dmso-d_6 at room temperature is ca. 5.1 × 10^3 Å, which is ca. four times larger than that of **1**-H$_3$ (ca. 1.3 × 10^3 Å). These results suggest that {Zn[**1**-H]}$_4$ adopts the same tetrameric structure in solution as in the solid state.

Factors that Influence the Structure of {Zn[1-H]}$_4$ and Implications for the Synthesis of Pd$_4$ Cage Catalysts. The key difference between the D4R structure of target **H** and the observed 2-dimensional structure of {Zn[1-H]}$_4$ is that in **H** the acidic hydrogen is located on the phosphine whereas in {Zn[**1**-H]}$_4$ the acidic hydrogen is located at the phosphonate oxygen and the phosphine binds to Zn. This result reflects the higher basicity of the phosphonate vs. the phosphine (cf. pK_a of PhPO$_3$H$^-$: 7.07; pK_a of PPh$_3$H$^+$: 2.7)[4a,16] and the softer character of Zn^{2+} vs. H^+. Importantly however, although {Zn[**1**-H]}$_4$ does not adopt a D4R structure, it has the correct composition and stereochemical configurations at the phosphine P atoms for the ultimate formation of the target D4R cage compound **G** (Chart 1). Therefore, its reactivity with Pd alkyl complexes was explored.

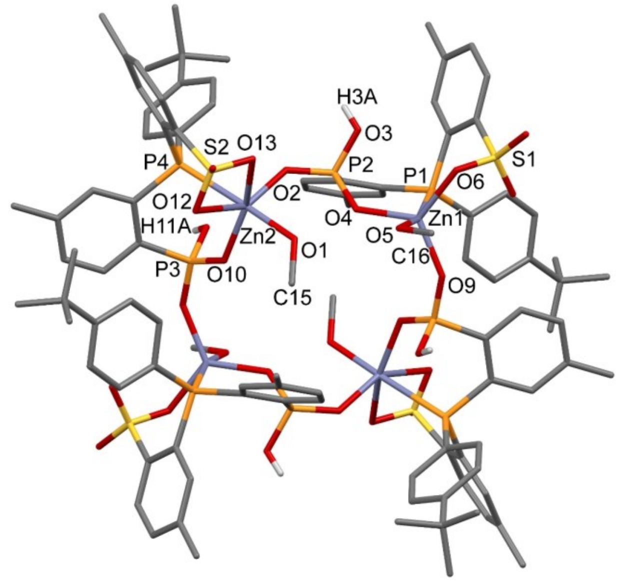

Figure 1. Molecular structure of {Zn[**1**-H](CH$_3$OH)}$_4$•12CH$_3$OH. Hydrogen atoms except acidic hydrogens and non-Zn^{2+}-coordinated CH_3OH molecules are omitted. Selected bond lengths (Å) and angles (deg): Zn1-O5 2.136(2), Zn2-O1 2.059(2), Zn1-O6 2.015(2), Zn2-O12 2.536(3), Zn2-O13 2.407(3), Zn1-P1 2.6115(9), Zn2-P4 2.4845(8), Zn1-O4 1.959(2), Zn1-O9 1.913(2), Zn2-O2 1.974(2), Zn2-O10 1.978(2), P2-O2 1.498(2), P2-O4 1.513(2), P3-O9 1.498(2), P3-O10 1.506(2), O9-Zn1-O4 120.01(9), O2-Zn2-O10 116.99(9), O2-P2-O4 112.96(12), O9-P3-O10 116.24(13).

Reaction of {Zn[1-H]}$_4$ with (TMEDA)PdMe$_2$. The reaction of {Zn[**1**-H]}$_4$•1.3CH$_3$OH with (TMEDA)PdMe$_2$ and pyridine in CD$_2$Cl$_2$, followed by the addition of Et$_2$O, yields {[(κ^2-*O*P-*P*-SO)PdMe(py)][Zn(TMEDA)]}$_2$•4CH$_2$Cl$_2$ (**2**•4CH$_2$Cl$_2$), which was identified by X-ray crystallography (Scheme 4 and Figure 2).[17] Compound **2** adopts a dimeric structure in which two (κ^2-*O*P-*P*-SO)PdMe(py) and two Zn(TMEDA) units are linked by 3.111-bridging phosphonates to form a central Zn$_2$P$_2$O$_4$ ring. The phosphonate bridges and Zn$_2$P$_2$O$_4$ ring are similar to those of **C** and **B**, respectively (Chart 1).[6d] The phosphine P atoms have *RS* configurations and the overall symmetry is C_i. The pendant (aryl)SO_3^- group is positioned above the Pd square plane at the van der Waals contact distance (d(Pd1-O4) = 3.146 Å; sum of Pd and O van der Waals radii = 3.15 Å) and forms H-bonds with the CH$_2$Cl$_2$ solvent molecules. Similar arrangements of pendant ArSO$_3^-$ groups in Pd catalysts have been reported previously.[1a,18]

A likely reason for formation of dimeric **2** rather than a tetrameric product with a D4R structure is that the TMEDA ligands occupy two coordination sites at the Zn^{2+} centers, which prevents the coordination of a third ArPO$_3^{2-}$ ligand to generate a Zn$_4$P$_4$O$_{12}$ cage.

Reaction of {Zn[1-H]}$_4$ with (COD)PdMe$_2$ to Form Pd$_4$ Compounds with D4R Zn$_4$P$_4$O$_{12}$ Cores. To avoid the presence of ligands that might coordinate to Zn^{2+} and prevent D4R cage formation, (COD)PdMe$_2$ (COD = 1,5-cyclooctadiene) was utilized as the Pd source in a reaction with {Zn[**1**-H]}$_4$. Coordination of COD to Zn^{2+} is unlikely due to the poor back-bonding ability of Zn(II), and zinc-olefin complexes are rare.[19]

Scheme 3. Synthesis of {Zn[1-H]}$_4$. Ar = 4-^{t}Bu-Ph. The lower phosphonium-phosphonate-sulfonate units in H are denoted by "PH$^+$".

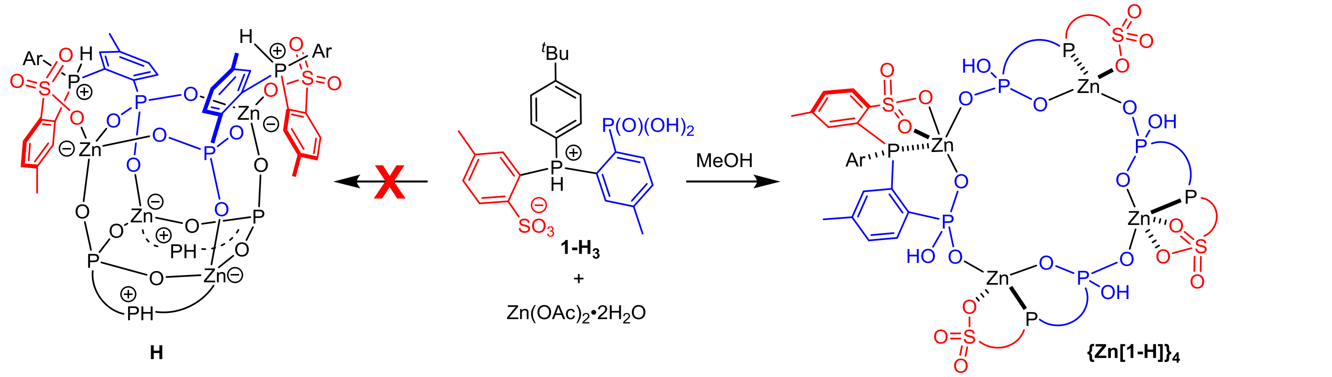

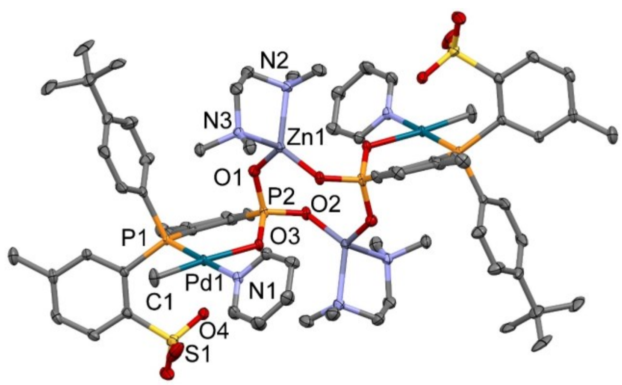

Figure 2. Molecular structure of **2**•4CH_2Cl_2. Hydrogen atoms and CH_2Cl_2 solvent molecules are omitted. Selected bond lengths (Å) and angles (deg): Pd1-C1 2.030(5), Pd1-N1 2.104(4), Pd1-O3 2.126(3), Pd1-P1 2.2136(13), Zn1-O2 1.907(3), Zn1-O1 1.928(3), Zn1-N2 2.068(4), Zn1-N3 2.087(4), P2-O1 1.515(4), P2-O2 1.521(3), P2-O3 1.519(3), C1-Pd1-N1 89.08(19), C1-Pd1-O3 174.16(19), N1-Pd1-O3 85.20(13), C1-Pd1-P1 89.80(16), N1-Pd1-P1 177.57(11), O3-Pd1-P1 95.96(9), O2-Zn1-O1 117.22(14), N2-Zn1-N3 87.08(16), O1-P2-O2 111.57(19).

The sequential reaction of CH_3OH-free {Zn[**1**-H]}$_4$ with (COD)PdMe$_2$ and 4-^{t}Bu-pyridine in CD_2Cl_2 affords {[κ^2-(Zn-OP-*P*-S*O*)]PdMe(4-^{t}Bu-py)}$_4$ (**4**-(4-^{t}Bu-py)) as the major product (>80%, Scheme 4). **4**-(4-^{t}Bu-py) was isolated in analytically pure form by recrystallization from $CHCl_2CHCl_2$/toluene/pentane solution at -40 °C and X-ray quality crystals were obtained by crystallization from $CHCl_2CHCl_2$ at room temperature. X-ray crystallographic analysis shows that **4**-(4-^{t}Bu-py) adopts the target D4R $Zn_4P_4O_{12}$ cage structure (Figure 3). The [OP-P-SO]$^{3-}$ ligand chelates to Pd through the phosphine and sulfonate groups, and the pendant phosphonate group forms the D4R cage through 3.111 bridges to the Zn^{2+} ions. The Zn^{2+} corners are capped by sulfonate oxygens. The four Pd units are arranged in two pairs with *SS* and *RR* configurations at the phosphine P atoms and the overall structure has approximate S_4 symmetry. The Pd-Me groups lie in close proximity to the 4-^{t}Bu-py ring of the neighboring Pd unit (Figure 3b). The four "side" faces of the cage are blocked by arenesulfonate groups. The key cage dimensions of **4**-(4-^{t}Bu-py) and **A$_4$** are summarized in Table 1 and are quite similar.

NMR spectra of analytically pure **4**-(4-^{t}Bu-py) (obtained by recrystallization from $CHCl_2CHCl_2$/toluene/pentane as noted above) contain major resonances (>80%) that are consistent with the *SSRR* diastereomer identified by X-ray crystallography. The ^{1}H NMR spectrum of the major species exhibits only one set of OP-P-SO ligand resonances, indicating that it is highly symmetric, and contains a Pd-Me resonance at δ -0.20 (d, J_{PH} = 3 Hz). The high-field shift of the Pd-Me resonance is consistent with anisotropic shielding by an adjacent py ring, and the small J_{PH} value indicates a *cis* arrangement of the phosphine and methyl ligands.[2q,20] The ^{31}P{^{1}H} NMR spectrum contains two singlets at δ 36.4 (phosphine) and δ 9.4 (phosphonate) consistent with a (κ^2-OP-*P*-S*O*)Pd coordination mode.[21] In addition, the ^{1}H spectrum contains two sets of minor Pd-Me resonances (total <20%) comprising in each case four equal intensity signals (d, J_{PH} = 1-7 Hz). The minor species giving rise to these resonances have not been conclusively identified but are likely to be diastereomers of **4**-(4-^{t}Bu-py) with different relative configurations at the phosphine P atoms (see Supporting Information).

Table 1. Comparison of Metrical Parameters for 4-(4-^{t}Bu-py) and A$_4$.

Parameter	**4**-(4-^{t}Bu-py)		**A$_4$**^{b}	
Edge (Å)	Zn---P	3.19(4)	Li---S	3.21(2)
Face diagonal (Å)	P---P	4.72(11)	S---S	4.62 (10)
	Zn---Zn	4.28(9)	Li---Li	4.45 (7)
Body diagonal (Å)	Zn---P	5.51(3)	Li---S	5.55
Pd-Pd (Å)^a		6.26(14)	Pd---Pd	6.04
Angle between Pd planes (deg)^a		74.86 (2.06)		73.96

^{a} within each pair of proximal Pd units. ^{b} ref 1.

Heating a solution of **4**-(4-^{t}Bu-py) in $CDCl_2CDCl_2$ to 80 °C does not produce significant changes in the ^{31}P{^{1}H} or ^{1}H NMR spectra, indicating that **4**-(4-^{t}Bu-py) is thermally robust and, in contrast to **A$_4$**, does not undergo significant cage disassembly under these conditions. However, **4**-(4-^{t}Bu-py) reacts with excess 4-^{t}Bu-py in CD_2Cl_2 over several hours at room temperature to form a mixture of unknown species.[22]

The reaction of CH_3OH-free {Zn[**1**-H]}$_4$ with (COD)PdMe$_2$ and pyridine gave similar results, although a crystalline product could not be obtained in this case. As for **4**-(4-^{t}Bu-py), the NMR spectra of **4**-py contain major resonances (>80 % of total intensity) consistent with the S_4-symmetric *SSRR* diastereomer and minor resonances attributed to other stereoisomers. Key NMR resonances for the major species include

Scheme 4. Synthesis of 2, 4-L and 3-L. Ar = 4-^{t}Bu-Ph. The lower (phosphine-sulfonate)PdMe(L) units in 4-L are denoted by "Pd".

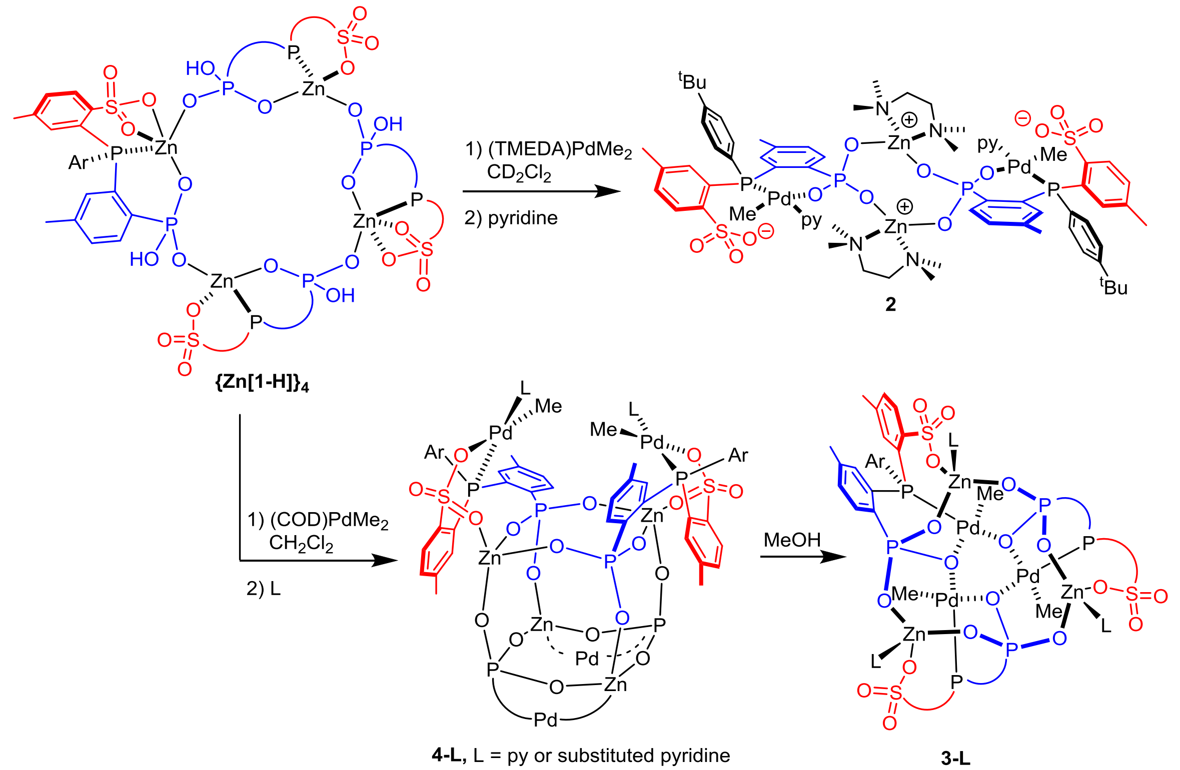

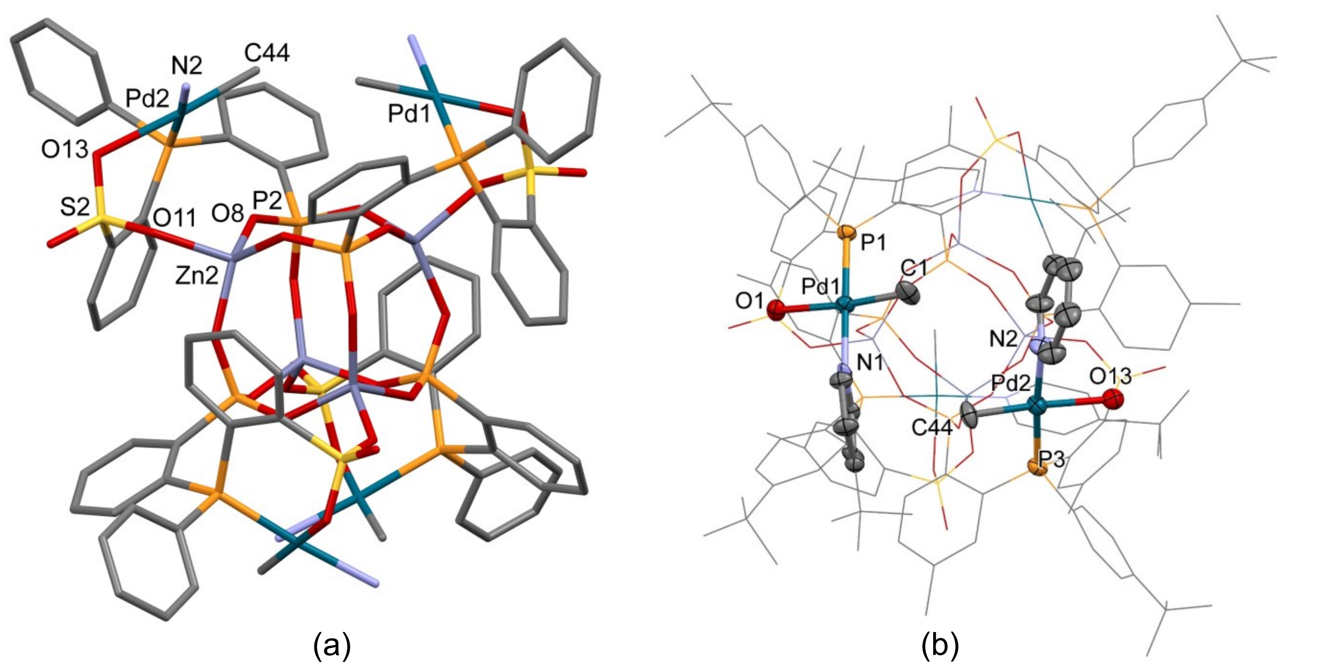

Figure 3. (a) Molecular structure of **4**-(4-^{t}Bu-py). Hydrogen atoms and the Me and ^{t}Bu substituents on the aryl groups are omitted. Only the nitrogen atom of the 4-^{t}Bu-py group is shown. Selected bond lengths (Å) and angles (deg): Pd2-C44 2.032(16), Pd2-N2 2.081(14), Pd2-O13 2.229(11), Pd2-P3 2.230(5), S2-O13 1.476(11), S2-O11 1.471(11), Zn2-O11 2.019(10), Zn2-O8 1.918(10), P2-O8 1.507(10), C44-Pd2-N2 91.4(6), C44-Pd2-O13 175.4(6), N2-Pd2-O13 91.6(5), C44-Pd2-P3 93.4(5), N2-Pd2-P3 175.2(4), O13-Pd2-P3 83.7(3). (b) View of **4**-(4-^{t}Bu-py) highlighting the orientation of the Pd-Me and 4-^{t}Bu-py units. Hydrogen atoms are omitted.

singlets at δ 35.5 (phosphine) and δ 8.8 (phosphonate) in the $^{31}P\{^1H\}$ spectrum and a Pd-Me resonance at δ -0.20 (d, J_{PH} =3 Hz) in the ^1H spectrum. PGSE-NMR analysis of the major Pd-Me resonance in CD_2Cl_2 at room temperature shows that the hydrodynamic volume of **4**-py is 6.5 × 10^3 Å, which is very similar to that for $\mathbf{A_4}$ (6.2×10^3 Å). Similar results were obtained with other pyridine ligands.

Reaction of 4-py with CH_3OH to Produce a Trimeric Pd_3 Cluster. Dissolution of **4**-py in CH_3OH at room temperature results in complete conversion to the trimeric species {(κ^2-Zn(py)-*O*P-*P*-SO)PdMe}$_3$ (**3**-py, Scheme 4), which crystallizes as **3**-py•0.5CH_3OH from the CH_3OH solution. The structure of **3**-py was determined by X-ray diffraction and is shown in Figure 4 and schematically in Scheme 4. **3**-py adopts a cage structure composed of $Zn_3P_3O_6$ and Pd_3O_3 rings that are linked through 4.211-bridging (aryl)PO_3^{2-} groups analogous to those in **E**. The Zn atoms have distorted tetrahedral geometry and lie at the van der Waals contact distance from the proximal Pd atoms (*d*(Zn-Pd) = 3.026 Å; sum of Zn and Pd van der Waals radii = 3.02 Å). The coordination geometry at Pd is square-planar and the Pd-Me group is buried in a deep pocket formed by the arene rings of the $[OP\text{-}P\text{-}SO]^{3-}$ ligand (Figure 5). Other **4**-L compounds react with CH_3OH in the same manner.

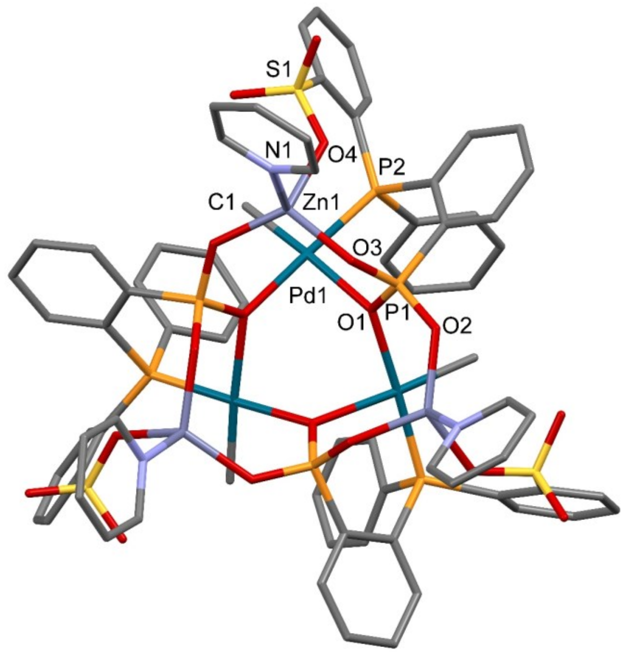

Figure 4. Molecular structure of **3**-py•0.5CH_3OH. Hydrogen atoms, Me and ^{t}Bu substituents on the aryl rings, and the CH_3OH molecule are omitted. Selected bond lengths (Å) and angles (deg): Pd1-C1 2.007(9), Pd1-O1 2.104(5), Pd1-P2 2.197(2), Zn1-O2 1.921(5), Zn1-O3 1.916(6), Zn1-O4 1.957(6), Zn1-N1 1.981(7), Zn1-Pd1 3.0265(17), S1-O4 1.467(6), P1-O1 1.541(6), P1-O2 1.510(5), P1-O3 1.516(6), C1-Pd1-O1 90.3(3) and 176.0(3), O1-Pd1-O1 87.9(3), C1-Pd1-P2 92.5(3), P2-Pd1-O1 89.45(15) and 176.48(17), Pd1-O1-Pd1 125.3(3), O3-Zn1-O2 117.1(2), O2-P1-O3 111.8(4), P1-O2-Zn1 130.7(3), P1-O3-Zn1 131.7(4).

The pyridine ligand of **3**-py is labile. Isolation of **3**-py on a preparatory scale by filtration, washing with CH_3OH, and drying under vacuum afforded a sample that contained 0.85 equiv of pyridine per Pd-Me unit. The $^{31}P\{^1H\}$ and ^1H NMR spectra of this material were broad but sharpened upon the addition of excess pyridine.[23] Exchange of the pyridine ligand of **3**-py with free pyridine is fast on the NMR time scale at room temperature. The $^{31}P\{^1H\}$ NMR spectrum of **3**-py in CD_2Cl_2 in the

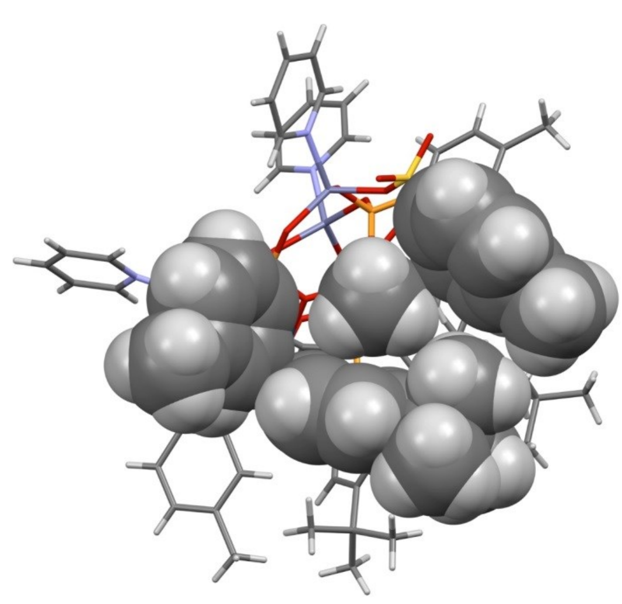

Figure 5. View of **3**-py highlighting the steric crowding of the Pd-Me groups by the arene rings of the$[OP\text{-}P\text{-}SO]^{3-}$ ligand.

presence of excess pyridine contains two doublets at δ 42.7 (phosphine) and 19.4 (phosphonate) with J_{PP} = 12 Hz, consistent with the (OS-*P*-P*O*)Pd chelation observed in the solid-state structure.[21] The Pd-Me ^1H NMR resonance appears at unusually high-field (δ -0.81), consistent with the anisotropic shielding expected from the solid-state structure. The hydrodynamic volume of **3**-py determined by PGSE-NMR in CD_2Cl_2 at 25 °C (4.5×10^3 Å) is ca. ¾ of the value for **4**-py (6.5×10^3 Å). Therefore, the solution structure must be very similar to the solid-state structure. The NMR spectra of **3**-py in $CDCl_2CDCl_2$ solution are unchanged up to 80 °C, indicating that **3**-py is thermally robust.[24]

The sensitivity of **4-L** compounds to CH_3OH requires that CH_3OH-free {Zn[**1**-H]}$_4$ be used in their synthesis. The reaction of {Zn[**1**-H]}$_4$•1.6 CH_3OH with (COD)$PdMe_2$ and pyridine in CD_2Cl_2 produced a mixture of **4**-py and **3**-py.

Base-free Complexes Derived from 4-(4-^{t}Bu-py) and 3-py. The reaction of **4**-(4-^{t}Bu-py) (ca. 80 % major isomer) with $B(C_6F_5)_3$ in CD_2Cl_2 at room temperature generates (py)$B(C_6F_5)_3$ and a poorly-soluble species presumed to be a base-free complex derived by loss of 4-^{t}Bu-py from **4**-(4-^{t}Bu-py). Addition of 1 equiv of 4-^{t}Bu-py to the base-free complex in CD_2Cl_2 at room temperature regenerates **4**-(4-^{t}Bu-py) in 39 % yield along with minor stereoisomers (total 61 %), suggesting that base-free **4** is susceptible to isomerization. Similarly, the reaction of **3**-py with $B(C_6F_5)_3$ in $CDCl_2CDCl_2$ generates (py)$B(C_6F_5)_3$ and a poorly-soluble base-free species. In this case however, addition of pyridine to the base-free complex regenerates **3**-py in 96 % yield.

Ethylene Polymerization. The ethylene polymerization behavior of **4**-(4-^{t}Bu-py) and **3**-py was examined. A sample of **4**-(4-^{t}Bu-py) that contained ca. 80 % of the major stereoisomer was used for polymerization studies. $B(C_6F_5)_3$ was added to trap the 4-^{t}Bu-py ligand, in order to minimize cage decomposition induced by the 4-^{t}Bu-py that is displaced by ethylene (*vide supra*). In the presence of 1 equiv of $B(C_6F_5)_3$ per Pd, **4**-(4-^{t}Bu-py) produces high-MW linear PE with a broad MWD at 80 ˚C in toluene/chlorobenzene solution and in hex-

Table 2. Ethylene Polymerization by 4-(4-^{t}Bu-py) and 3-py.[a]

Entry	Catalyst	T (°C)	Solvent (50 mL)	Yield (g)	Activity ($kg{\bullet}mol^{-1}{\bullet}h^{-1}$)	M_w[d] (10^3 Da)	M_w/M_n[d]	T_m[e] (°C)
1[b]	**4**-(4-^{t}Bu-py) + $B(C_6F_5)_3$	80	toluene/chloro-benzene (49/1)	4.74	237	436	15	136.9
2[b]	**4**-(4-^{t}Bu-py) + $B(C_6F_5)_3$	80	hexanes/chloro-benzene (49/1)	5.11	256	1031	6.6	135.4
3[b]	**3**-py	80	toluene	2.18	108	466	4.1	138.1
4[b]	**3**-py	25	CH_2Cl_2	0.14	7.1	1010	21	137.2
5[c]	**3**-py	25	CH_2Cl_2	0.53	4.4	1438	14	137.0
6[b]	**3**-py + $B(C_6F_5)_3$	80	toluene/chloro-benzene (49/1)	7.64	378	691	2.7	136.6

[a]P_{C2H4} = 410 psi, 1 equiv of $B(C_6F_5)_3$ per 4-^{t}Bu-pyridine or pyridine when applicable. [b]Time = 2 h, [Pd] = 10 μmol. [c] Time = 24 h, [Pd] = 5 μmol. [d]GPC. [e]DSC.

anes/chlorobenzene suspension (Table 2, entries 1, 2). The broad MWDs indicate that **4**-(4-^{t}Bu-py) functions as a multi-site catalyst in the presence of $B(C_6F_5)_3$, which is not surprising given the extensive cage isomerization observed for the base-free complex derived from **4**-(4-^{t}Bu-py) and $B(C_6F_5)_3$. The ethylene polymerization performance of **4**-(4-^{t}Bu-py) is similar to that of $\mathbf{A_4}$ and its analogues.[1,3]

A sample of **3**-py that contained 0.85 equiv of pyridine per Pd was used for ethylene polymerization studies. $B(C_6F_5)_3$ was not required in this case as **3**-py is stable in the presence of excess pyridine. In toluene at 80 ˚C, **3**-py produces high-MW linear PE with a moderately broad MWD (Table 2, entry 3). The broadening of the MWD may result from the presence of active species that maintain the core structure of **3**-py but contain different numbers of pyridine ligands. Consistent with this explanation, in the presence of 1 equiv of $B(C_6F_5)_3$ per pyridine in toluene at 80 ˚C, **3**-py exhibits increased activity and yields high-MW linear PE with a narrow MWD (Table 2, entry 6), characteristic of a single-site catalyst.

CONCLUSION

The phosphine-phosphonate-sulfonate proligand HP^+(4-^{t}Bu-Ph)(2-PO_3H_2-5-Me-Ph)(2-SO_3^--5-Me-Ph) (H_3[OP-P-SO], **1**-H_3) functions as a building block for the self-assembly of multinuclear Pd compounds based on zinc phosphonate scaffolds. The reaction of **1**-H_3 with $Zn(OAc)_2{\bullet}2H_2O$ yields {Zn[**1**-H]}$_4$, which adopts a 2-dimensional $Zn_4P_4O_8$ ring structure. The higher basicity of the phosphonate group versus the phosphine favors this structure over a D4R cage structure. The sequential reaction of CH_3OH-free {Zn[**1**-H]}$_4$ with (COD)$PdMe_2$ and 4-^{t}Bu-py generates {[κ^2-*P,SO*-(Zn-OP-*P*-S*O*)]PdMe(4-^{t}Bu-py)}$_4$ (**4**-^{t}Bu-py), which adopts a tetrameric structure in which four [OP-*P*-S*O*)]PdMe(4-^{t}Bu-py)$^{2-}$ units are arranged on the periphery of a D4R $Zn_4P_4O_{12}$ cage and the phosphine P atoms have *SSRR* configurations. The $^{31}P\{^1H\}$ and ^1H NMR spectra of **4**-(4-^{t}Bu-py) are consistent with the solid-state structure and are unchanged up to 80 °C, indicating that **4**-(4-^{t}Bu-py) is resistant to cage disassembly under these conditions. Two sets of minor Pd-Me ^1H NMR resonances are present in the ^1H NMR spectrum of **4**-(4-^{t}Bu-py) and are assigned to stereoisomers. Analogous **4**-**L** species were generated by the reaction of {Zn[**1**-H]}$_4$, (COD)$PdMe_2$ and other pyridine ligands and exhibit similar properties. **4**-py reacts with CH_3OH to form a trimeric cluster **3**-py, which adopts a cage structure composed of $Zn_3P_3O_6$ and Pd_3O_3 rings linked through 4.211-bridging (aryl)PO_3^{2-} groups. **4**-(4-^{t}Bu-py) decomposes in the presence of excess 4-^{t}Bu-py. In the presence of 1 equiv of $B(C_6F_5)_3$ per 4-^{t}Bu-pyridine at 80 ˚C in toluene or in a hexanes suspension, **4**-(4-^{t}Bu-py) produces high-MW linear PE with a broad MWD, characteristic of multi-site catalysis. In contrast, in the presence of 1 equiv of $B(C_6F_5)_3$ per pyridine at 80 ˚C in toluene, **3**-py produces high-MW linear PE with a narrow MWD, characteristic of single-site catalysis. While Zn-phosphonate cage compound **4**-(4-^{t}Bu-py) is much more thermally stable than Li-sulfonate analogue $\mathbf{A_4}$, its reactivity with Lewis bases (py, CH_3OH) limits its utility as a catalyst and mechanistic probe. New strategies will be required to design multinuclear D4R-cage-based catalysts that are both thermally and chemically stable.

EXPERIMENTAL SECTION

General procedures. All experiments were performed under a nitrogen atmosphere using drybox or Schlenk techniques. Nitrogen was purified by passage through Q-5 oxygen scavenger and activated molecular sieves. CH_2Cl_2, Et_2O and THF were dried by passage over activated alumina. Toluene, pentane and hexane were purified by passage through BASF R3-11 oxygen scavenger and activated alumina. $CDCl_2CDCl_2$, CH_2ClCH_2Cl and $CHCl_2CHCl_2$ were dried over 4 Å molecular sieves. CD_2Cl_2 was dried over P_2O_5. The following compounds were prepared by literature procedures: (4-^{t}Bu-Ph)PCl_2,[1] diethyl (2-bromo-4-tolyl)phosphonate,[18,21a,25,26] (TMEDA)$PdMe_2$,[27] (COD)$PdMe_2$.[28] *para*-toluenesulfonic acid (Aldrich, monohydrate) was dried by azeotropic distillation in benzene. 4-^{t}Bu-pyridine (Aldrich) was purified by vacuum distillation. Other reagents were obtained from commercial sources and used without purification. The synthesis of **1**-H_3 is described in the Supporting Information. Elemental analyses were performed by Robertson Microlit Laboratories. The solvent content in elemental analysis samples was quantified by ^1H NMR. NMR spectra were acquired on Bruker DRX-500 or Bruker DRX-400 spectrometers at ambient temperatures unless otherwise indicated. ^1H and ^{13}C chemical shifts are reported relative to $SiMe_4$ and are internally referenced to residual ^1H and ^{13}C solvent resonances. ^{31}P chemical shifts are reported relative to externally referenced 85% H_3PO_4. ^{19}F spectra were referenced to external $BF_3{\bullet}Et_2O$, and ^{19}F chemical shifts are reported relative to $CFCl_3$. Coupling constants are reported in Hz. NMR resonances were assigned based on COSY, NOESY, HMQC, HMBC and $^1H\{^{31}P\}$ experiments, as well as trends in chemical shifts and coupling constants derived from these experiments. Mass spectrometry was performed on Agilent 6224 TOF-MS (high resolution) or Agilent 6130 LCMS (low resolution) instruments.

Ethylene polymerization reactions were performed in a Parr 300 mL stainless steel autoclave, which was equipped with a mechanical stirrer, thermocouple and water cooling loop and controlled by a Parr 4842 controller. Gel permeation chromatography (GPC) data were obtained on a Polymer Laboratories PL-GPC 220 instrument at 150 °C with 1,2,4-trichlorobenzene (stabilized with 125 ppm BHT) as the mobile phase. Three PLgel 10 μm Mixed-B LS columns were used. Molecular weights were calibrated using narrow polystyrene standards (ten-point calibration with M_n from 570 Da to 5670 kDa) and are corrected for linear polyethylene by universal calibration using the following Mark-Houwink parameters: polystyrene, K = 1.75 $\times 10^{-2}$ cm^3g^{-1}, α = 0.67; polyethylene, K = 5.90 $\times 10^{-2}$ cm^3g^{-1}, α = 0.69.[29] DSC measurements were performed on a TA Instruments DSC 2920 instrument. Samples (10 mg) were annealed by heating to 170 °C at 20 °C/min, cooled to 40 °C at 20 °C/min, and then analyzed while being heated to 170 °C at 20 °C/min.

{Zn[H(OP-P-SO)]}$_4$ ({Zn[1-H]}$_4$). A Schlenk flask was charged with **1-H$_3$** (0.71 g, 1.4 mmol), $Zn(OAc)_2$•$2H_2O$ (0.31 g, 1.4 mmol) and N_2-purged CH_3OH (70 mL) to yield a white suspension. CH_2Cl_2 (15 mL) was added by syringe until the solution became clear. The mixture was stirred at room temperature for 2 h, concentrated under vacuum to ca. 50 mL, and left at room temperature for 18 h without stirring to precipitate {Zn[**1**-H]}$_4$ out of solution. The product was isolated by filtration and washed with CH_3OH to afford a white solid. The product was heated to 50 ˚C for 2 d under vacuum to yield CH_3OH-free {Zn[**1**-H]}$_4$ (0.67 mg, 84 %). X-ray quality crystals of {Zn[**1**-H]}$_4$•16CH_3OH were grown from CH_3OH solution at room temperature. $^{31}P\{^1H\}$ NMR (DMSO-d_6): δ 12.2 (br s, *P*=O), -17.7 (s, Zn-*P*). ^1H NMR (DMSO-d_6): δ 10.6 (br, 1H, -O*H*), 7.82 (br, 2H, H^3 and H^9), 7.31-7.27 (br, 4H, H^4, H^{10} and H^{15}), 6.96 (br, 2H, H^6 and H^{12}), 6.80 (br, 2H, H^{14}), 2.19 (s, 6H, H^{17} and H^{18}), 1.25 (s, 9H, H^{20}). $^{13}C\{^1H\}$ NMR (DMSO-d_6): δ 151.4 (br), 146.6 (br), 146.4 (br), 139.7 (br), 139.1 (br), 135.6 (s), 134.8 (d, J_{PC} = 12), 133.1 (d, J_{PC} = 15), 130.2 (br), 129.8 (br), 127.3 (s), 124.9 (d, J_{PC} = 7), 34.4 (s, C^{19}), 31.0 (s, C^{20}), 21.1 (s, C^{18}), 20.9 (s, C^{17}). Four carbon resonances were not observed due to the broadness of the spectrum and possible overlapping among resonances. HRMS (*m/z*): Calcd. for $[C_{96}H_{104}Zn_4O_{24}P_8S_4 - Zn + 3H]^+$ 2217.1668, Found: 2217.1676. When the product was dried under vacuum at room temperature for 1 d, (instead of at 50 ˚C for 2 d), the isolated material contained ca. 1.3 equiv CH_3OH per {Zn[**1**-H]}$_4$.

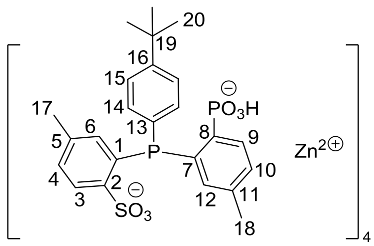

Figure 6. NMR labeling scheme for {Zn[**1**-H]}$_4$.

{[(κ^2-*OP*-*P*-SO)PdMe(py)][Zn(TMEDA)]}$_2$ (2). A vial was charged with {Zn[**1**-H]}$_4$•1.3CH_3OH (49 mg, 0.020 mmol), (TMEDA)$PdMe_2$ (21 mg, 0.020 mmol) and CH_2Cl_2 (1 mL). The yellow solution was stirred at room temperature for 1 h. Pyridine (6.8 μL, 0.020 mmol) was added, and the solution was stirred for an additional 18 h. The mixture was filtered through Celite, and Et_2O was diffused into the filtrate at room temperature to afford colorless crystals (10 mg, 23 %) that were identified as **2**•4CH_2Cl_2 by X-ray crystallography. The NMR spectra of **2** in CD_2Cl_2 are very complicated and the speciation of this compound in solution could not be established. EA: Calcd. for $[C_{36}H_{49}N_3O_6P_2PdSZn]_2$•$4CH_2Cl_2$, %: C, 43.24; H, 5.06; N, 3.98; Zn, 6.20; Pd, 10.08. Found: C, 46.92; H, 5.33; N, 3.88; Zn, 6.28; Pd, 8.39. Although the Pd and C results are outside the range viewed as establishing analytical purity, they are provided to illustrate the best values obtained to date

4-(4-^{t}Bu-py). A vial was charged with CH_3OH-free {Zn[**1**-H]}$_4$ (0.18 g, 0.31 mmol), (COD)$PdMe_2$ (77 mg, 0.31 mmol) and CH_2Cl_2 (5 mL). The mixture was stirred at room temperature for 1 h to afford a yellow solution. 4-^{t}Bu-py (46 μL, 0.31 mmol) was added, and the mixture was stirred for an additional 18 h. The mixture was filtered through Celite and the volatiles were removed under vacuum to afford a yellow solid. The solid was recrystallized by layering pentane onto a $CHCl_2CHCl_2$/toluene solution and cooling to -40 °C. **4**-(4-^{t}Bu-py) was collected by filtration and dried under vacuum for 18 h (122 mg, 77 %). $^{31}P\{^1H\}$ NMR (CD_2Cl_2): δ 36.4 (s, Pd-*P*), 9.4 (s, *P*=O). ^1H NMR (CD_2Cl_2): δ 8.54 (d, $^3J_{HH}$ = 5, 2H, H^{17}), 8.29 (m, 1H, H^9), 7.80 (dd, $^3J_{HH}$ = 8, $^4J_{PH}$ = 5, 1H, H^3), 7.63 (d, $^3J_{HH}$ = 8, 1H, H^{10}), 7.60 (d, $^3J_{HH}$ = 8, 1H, H^4), 7.46-7.44 (br, 4H, H^{14} and H^{15}; the H^{14} resonance is broadened due to the restricted rotation around the P-C^{13} bond), 7.23 (d, $^3J_{PH}$ = 12, 1H, H^6), 6.81 (d, $^3J_{HH}$ = 6, 2H, H^{18}), 6.61 (dd, $^3J_{PH}$ = 12, $^4J_{PH}$ = 4, 1H, H^{12}), 2.48 (s, 3H, H^{20}), 2.31 (s, 3H, H^{21}), 1.38 (s, 9H, H^{25}), 1.15 (s, 9H, H^{23}), -0.29 (d, $^3J_{PH}$ = 3, 3H, Pd-C*H*$_3$). $^{13}C\{^1H\}$ NMR (CD_2Cl_2): δ 161.8 (s), 154.4 (s), 151.3 (s), 142.5 (d, J_{PC} = 7), 141.5 (d, J_{PC} = 12), 140.6 (d, J_{PC} = 13), 139.9 (d, J_{PC} = 10), 138.8 (m), 136.9 (m), 134.9 (s), 134.6 (m), 131.3 (d, J_{PC} = 32), 131.0 (s), 130.4 (d, J_{PC} = 10), 130.1 (s), 129.6 (s), 129.2 (s), 126.0 (br), 122.0 (s), 35.1 (s), 35.0 (s), 31.3 (s), 30.3 (s), 21.8 (s), 21.5 (s), 0.2 (s, Pd-*C*H$_3$). EA: Calcd. for $[C_{34}H_{41}NO_6P_2PdSZn]_4$•2.18$CHCl_2CHCl_2$ (solvent content determined by ^1H NMR), %: C, 45.95; H, 4.63; N, 1.53; Zn, 7.13; Pd, 11.6. Found: C, 45.70; H, 4.32; N, 1.38; Zn, 7.60; Pd, 10.77. Although the Zn and Pd results are outside the range viewed as establishing analytical purity, they are provided to illustrate the best values obtained to date. X-ray quality crystals were grown by slow evaporation of a $CHCl_2CHCl_2$ solution at room temperature.

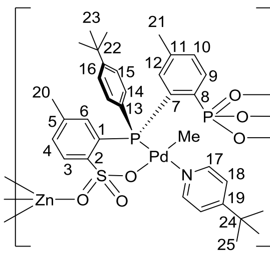

Figure 7. NMR labeling scheme for **4**-(4-^{t}Bu-py).

3-py. A vial was charged with CH_3OH-free {Zn[**1**-H]}$_4$ (0.11 mg, 0.20 mmol), (COD)$PdMe_2$ (49 mg, 0.20 mmol) and CH_2Cl_2 (5 mL), and the mixture was stirred at room temperature for 1 h to afford a clear yellow solution. Pyridine (16 μL, 0.20 mmol) was added, and the mixture was stirred for an additional 18 h. The mixture was filtered through Celite and the volatiles were removed under vacuum to afford **4**-py as a yellow solid. The solid was dissolved in N_2-purged CH_3OH (5 mL). The solution was left at room temperature for 18 h and yellow crystals formed. The crystals were collected by filtration and dried under vacuum for 18 h (82 mg, 54 %, the pyridine content was 0.85 equiv per Pd as determined by ^1H NMR in CD_2Cl_2/CD_3OD). $^{31}P\{^1H\}$ NMR (CD_2Cl_2/CD_3OD): δ 42.7 (d, J_{PP} = 12 Hz, Pd-*P*), 19.4 (d, J_{PP} = 12 Hz, *P*=O). ^1H NMR (CD_2Cl_2/CD_3OD): δ 8.87 (dd, $^3J_{PH}$ = 15, $^3J_{HH}$ = 8, 1H, H^3), 8.55 (d, $^3J_{HH}$ = 4, 2H, H^{17}), 8.22 (d, $^3J_{HH}$ = 8, 1H, H^4), 7.91-7.80 (m, 3H, H^9, H^{19} and $H^{14'}$), 7.43 (t, $^3J_{HH}$ = 6, 2H, H^{18}), 7.29-7.22 (m, 3H, H^{15} and H^{10}), 6.99 (t, $^3J_{PH}$ = $^3J_{HH}$ = 8, 1H, H^{14}), 6.89 (dd, $^3J_{PH}$ = 11, $^4J_{PH}$ = 4, 1H, H^{12}), 6.44 (d, $^3J_{PH}$ = 13, 1H, H^6), 2.20 (s, 3H, H^{20}), 2.09 (s, 3H, H^{21}), 1.28 (s, 9H, H^{23}), -0.84 (d, $^3J_{PH}$ = 2, 3H, Pd-C*H*$_3$). $^{13}C\{^1H\}$ NMR (CD_2Cl_2/CD_3OD): δ 155.7 (s, C^{16}), 149.5 (s, C^{17}), 143.9 (d, $^4J_{PC}$ = 9), 140.9 (d, $^4J_{PC}$ = 2, $C^{4'}$), 140.8 (d, J_{PC} = 9), 140.6 (d, J_{PC} = 29, C^3), 140.1 (dd, J_{PC} = 8, 3), 139.1 (d, J_{PC} = 8, C^{19}), 138.1 (dd, J_{PC} = 187, 18), 135.3 (d, J_{PC} = 14, C^{12}), 135.1 (d, J_{PC} = 7, C^6), 134.1 (s, C^{14}), 133.1 (dd, J_{PC} = 11, 7), 132.1 (s, C^{15}), 132.0 (d, J_{PC} = 11), 131.5 (dd, J_{PC} = 13, 2, C^{10}), 130.7 (d, J_{PC} = 7, $C^{14'}$), 127.5 (dd, J_{PC} = 199, 49), 127.2 (d, J_{PC} = 7), 125.4 (s, C^4), 125.3 (d, J_{PC} = 3, C^{18}), 35.4 (s, C^{22}), 31.1 (s, C^{23}), 21.3 (s, C^{20} and C^{21}), 1.5 (s, Pd-*C*H$_3$). EA: Calcd. for $[C_{25}H_{28}O_6P_2PdSZn$•$0.55CH_2Cl_2$•$0.81C_5H_5N]_3$ (solvent content determined by ^1H NMR), %: C, 44.39; H, 4.17; N, 1.42. Found: C, 44.61; H, 3.24; N, 1.57.

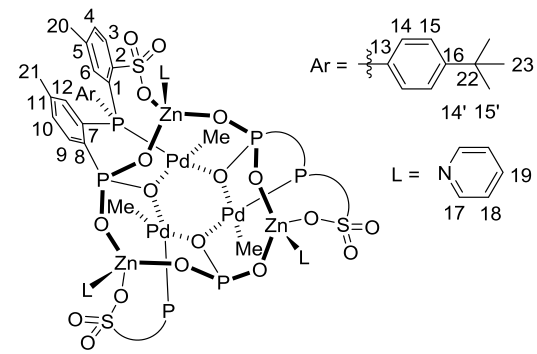

Figure 8. NMR labeling scheme for **3-py**.

ASSOCIATED CONTENT

Supporting Information

The Supporting Information is available free of charge on the ACS Publications website.

Additional experimental procedures and data, NMR spectra and supporting figures and tables (PDF)

Accession Codes: CCDC 1850964-1850967 and 1851601 contain the supplementary crystallographic data for this paper. These data can be obtained free of charge via www.ccdc.cam.ac.uk/data_request/cif, or by emailing data_request@ccdc.cam.ac.uk, or by contacting The Cambridge Crystallographic Data Centre, 12, Union Road, Cambridge CB2 1EZ, UK; fax: +44 1223 336033.

AUTHOR INFORMATION

Corresponding Author

* Email: rfjordan@uchicago.edu

Notes

The authors declare no competing financial interests.

ACKNOWLEDGMENT

This work was supported by the National Science Foundation (NSF) under grant number CHE-1709159. NSF's ChemMatCARS Sector 15 is principally supported by the Divisions of Chemistry (CHE) and Materials Research (DMR), NSF, under grant number CHE-1346572. Use of the Advanced Photon Source, an Office of Science User Facility operated for the U.S. Department of Energy (DOE) Office of Science by Argonne National Laboratory, was supported by the U.S. DOE under Contract No. DE-AC02-06CH11357. We thank Drs. Antoni Jurkiewicz, Alexander Filatov and C. Jin Qin for assistance with NMR, X-ray crystallography and mass spectrometry.

REFERENCES

1. (a) Shen, Z.; Jordan, R. F. Self-Assembled Tetranuclear Palladium Catalysts That Produce High Molecular Weight Linear Polyethylene. *J. Am. Chem. Soc.* **2010**, *132*, 52-53. (b) Shen, Z.; Jordan, R. F. Copolymerization of Ethylene and Vinyl Fluoride by (Phosphine-bis(arenesulfonate))PdMe(pyridine) Catalysts: Insights into Inhibition Mechanisms. *Macromolecules* **2010**, *43*, 8706-8708.

2. (a) Mitsushige, Y.; Yasuda, H.; Carrow, B. P.; Ito, S.; Kobayashi, M.; Tayano, T.; Watanabe, Y.; Okuno, Y.; Hayashi, S.; Kuroda, J., Okumura, Y.; Nozaki, K. Methylene-Bridged Bisphosphine Monoxide Ligands for Palladium-Catalyzed Copolymerization of Ethylene and Polar Monomers. *ACS Macro Lett.* **2018**, *7*, 305-311. (b) Nakano, R.; Chung, L. W.; Watanabe, Y.; Okuno, Y.; Okumura, Y.; Ito, S.; Morokuma, K.; Nozaki, K. Elucidating the Key Role of Phosphine−Sulfonate Ligands in Palladium-Catalyzed Ethylene Polymerization: Effect of Ligand Structure on the Molecular Weight and Linearity of Polyethylene. *ACS Catal.* **2016**, *6*, 6101-6113. (c) Liang, T.; Chen, C. Side-Arm Control in Phosphine-Sulfonate Palladium- and Nickel-Catalyzed Ethylene Polymerization and Copolymerization. *Organometallics* **2017**, *36*, 2338-2344. (d) Wu, Z.; Chen, M.; Chen, C. Ethylene Polymerization and Copolymerization by Palladium and Nickel Catalysts Containing Naphthalene-Bridged Phosphine–Sulfonate Ligands. *Organometallics* **2016**, *35*, 1472-1479. (e) Sui, X.; Dai, S.; Chen, C. Ethylene Polymerization and Copolymerization with Polar Monomers by Cationic Phosphine Phosphonic Amide Palladium Complexes. *ACS Catal.* **2015**, *5*, 5932-5937. (f) Nakano, R.; Nozaki, K. Copolymerization of Propylene and Polar Monomers Using Pd/IzQO Catalysts. *J. Am. Chem. Soc.* **2015**, *137*, 10934-10937. (g) Ota, Y.; Ito, S.; Kuroda, J.; Okumura, Y.; Nozaki, K. Quantification of the Steric Influence of Alkylphosphine–Sulfonate Ligands on Polymerization, Leading to High-Molecular-Weight Copolymers of Ethylene and Polar Monomers. *J. Am. Chem. Soc.* **2014**, *136*, 11898-11901. (h) Jian, Z. B.; Wucher, P.; Mecking, S. Heterocycle-Substituted Phosphinesulfonato Palladium(II) Complexes for Insertion Copolymerization of Methyl Acrylate. *Organometallics* **2014**, *33*, 2879-2888. (i) Carrow, B. P.; Nozaki, K. Transition-Metal-Catalyzed Functional Polyolefin Synthesis: Effecting Control through Chelating Ancillary Ligand Design and Mechanistic Insights. *Macromolecules* **2014**, *47*, 2541-2555. (j) Nakamura, A.; Anselment, T. M. J.; Claverie, J.; Goodall, B.; Jordan, R. F.; Mecking, S.; Rieger, B.; Sen, A.; van Leeuwen, P. W. N. M.; Nozaki, K. *Ortho*-Phosphinobenzenesulfonate: A Superb Ligand for Palladium-Catalyzed Coordination–Insertion Copolymerization of Polar Vinyl Monomers. *Acc. Chem. Res.* **2013**, *46*, 1438-1449. (k) Franssen, N. M. G.; Reek, J. N. H.; de Bruin, B. Synthesis of functional 'polyolefins': state of the art and remaining challenges. *Chem. Soc. Rev.* **2013**, *42*, 5809-5832. (l) Wucher, P.; Goldbach, V.; Mecking, S. Electronic Influences in Phosphinesulfonato Palladium(II) Polymerization Catalysts. *Organometallics* **2013**, *32*, 4516-4522. (m) Neuwald, B.; Falivene, L; Caporaso, L.; Cavallo, L.; Mecking, S. Exploring Electronic and Steric Effects on the Insertion and Polymerization Reactivity of Phosphinesulfonato Pd^{II} Catalysts. *Chem. Eur. J.* **2013**, *19*, 17773-17788. (n) Piche, L.; Daigle, J. C. Rehse, G.; Claverie, J. P. Structure–Activity Relationship of Palladium Phosphanesulfonates: Toward Highly Active Palladium-Based Polymerization Catalysts. *Chem. Eur. J.* **2012**, *18*, 3277-3285. (o) Carrow, B. P.; Nozaki, K. Synthesis of Functional Polyolefins Using Cationic Bisphosphine Monoxide–Palladium Complexes. *J. Am. Chem. Soc.* **2012**, *134*, 8802-8805. (p) Vela, J.; Lief, G. R.; Shen, Z.; Jordan, R. F. Ethylene Polymerization by Palladium Alkyl Complexes Containing Bis(aryl)phosphino-toluenesulfonate Ligands. *Organometallics* **2007**, *26*, 6624-6635. (q) Kochi, T.; Noda, S.; Yoshimura, K.; Nozaki, K. Formation of Linear Copolymers of Ethylene and Acrylonitrile Catalyzed by Phosphine Sulfonate Palladium Complexes. *J. Am. Chem. Soc.* **2007**, *129*, 8948-8949.(r) Skupov, K. M.; Marella, P. R.; Simard, M.; Yap, G. P. A.; Allen, N.; Conner, D.; Goodall, B. L.; Claverie, J. P. Palladium Aryl Sulfonate Phosphine Catalysts for the Copolymerization of Acrylates with Ethene. *Macromol. Rapid Commun.* **2007**, *28*, 2033-2038.

3. Pd_4 cage complexes based on PPh(2-SO_3Li-5-R-Ph)(2-SO_3^--5-R-Ph) ligands (R = ^{i}Pr, Cy, ^{t}Bu) that incorporate more strongly electron-ic-donating 5-R substituents on the arenesulfonate rings exhibit similar thermal stability and ethylene polymerization behavior as **A_4**. Wei, J.; Shen, Z.; Filatov, A. S.; Liu, Q.; Jordan, R. F. Self-Assembled Cage Structures and Ethylene Polymerization Behavior of Palladium Alkyl Complexes That Contain Phosphine-Bis(arenesulfonate) Ligands. *Organometallics* **2016**, *35*, 3557-3568.

4. Arenephosphonates are stronger bases than arenesulfonates (cf. pK_a of $PhPO_3H^-$: 7.07; pK_a of 4-Me-$PhSO_3H$: -2.8) and ligand binding constants are generally larger for Zn^{2+} than Li^+. (a) Jaffé, H. H.; Freedman, L. D.; Doak, G. O. The Acid Dissociation Constants of Aromatic Phosphonic Acids. I. Meta and Para Substituted Compounds. *J. Am. Chem. Soc.* **1953**, *75*, 2209-2211. (b) Guthrie, J. P. Hydrolysis of esters of oxy acids: pK_a values for strong acids;

Brønsted relationship for attack of water at methyl; free energies of hydrolysis of esters of oxy acids; and a linear relationship between free energy of hydrolysis and pK_a holding over a range of 20 pK units. *Can. J. Chem.* **1978**, *56*, 2342-2354. (c) Jensen, W. B. The Lewis acid-base definitions: a status report. *Chem. Rev.* **1978**, *78*, 1-22. (d) Deluchat, V.; Bollinger, J-C.; Serpaud, B.; Caullet, C. Divalent cations speciation with three phosphonate ligands in the pH-range of natural waters. *Talanta* **1997**, *44*, 897-907. (e) Sigel, H.; Chen, D.; Corfù, N.A.; Gregáň, F.; Holý, A.; Strakšá, M. Metal-ion-coordinating properties of various phosphonate derivatives, including 9-[2-(phosphonylmethoxy)ethyl]adenine (PMEA) - an adenosine monophosphate (AMP) analogue* with antiviral properties. *Helv. Chim. Acta* **1992**, *75*, 2634-2656. (f) Meisner, J.; Karwounopoulos, J.; Walther, P.; Kästner, J.; Naumann, S. The Lewis Pair Polymerization of Lactones Using Metal Halides and N-Heterocyclic Olefins: Theoretical Insights. *Molecules* **2018**, *23*, 432-446. (g) Remko, M.; Rode, B.M. Thermodynamics of binding of Li^+, Na^+, Mg^{2+} and Zn^{2+} to Lewis bases in the gas phase. *J. Mol. Struc.-Theochem* **2000**, *505*, 269-281.

5. Goura, J.; Chandrasekhar, V. Molecular Metal Phosphonates. *Chem. Rev.* **2015**, *115*, 6854-6965.

6. (a) Chandrasekhar, V.; Sahoo, D.; Metre, R. K. Isomorphic Co(II) and Zn(II) phosphonates: co-crystal formation of [{M_2(η^1-DMPzH)$_4$(Cl_3CPO_3)$_2$}{M(η^1-DMPzH)$_2$Cl2}$_2$](toluene)$_2$ (M = Co(II) and Zn(II)). *CrystEngComm* **2013**, *15*, 7419-7422. (b) Guo, L. R.; Bao, S. S.; Zheng, L. M. Self-assembly of two zinc complexes with flexible building block of 4-pyridylthioethylphosphonate. *Solid State Sci.* **2009**, *11*, 310-314. (c) Fan, Y. T.; Xue, D. X.; Li, G.; Hou, H. W.; Du, C. X.; Lu, H. J. Synthesis, crystal structures, and third-order nonlinear optical properties of two novel complexes of H4edbbp with Zn(II), Cd(II). *J. Mol. Struct.* **2004**, *707*, 153-160. (d) Howlader, R.; Walawalkar, M. G.; Murugavel, R. Mono and dinuclear group 12 phosphonates derived from a sterically encumbered phosphonic acid: Observation of esterification. *Inorg. Chim. Acta* **2013**, *405*, 147-154. (e) Xue, D.; Yin, M.; Fan, Y.; Zhu, A.; Lu, H.; Hou, H. Synthesis and crystal structure of a new zinc diphosphonate. *J. Coord. Chem.* **2005**, *58*, 1449-1454. (f) Ma, K-R.; Zhu, Y-L.; Yin, Q-F. Solvothermal synthesis and characterization of a new Zn^{II}-PMIDA phosphonate. *J. Coord.Chem.* **2009**, *62*, 3243-3249. (g) Chen, S-Pp.; Huang, G-X.; Li, M.; Pan, L-L; Yuan, Y-X.; Yuan, L-J. New *in Situ* Condensation Reaction of Amino Diphosphonic Acids: A Series of Bicyclic Phosphonate Derivatives and Three Novel Water Clusters. *Cryst. Growth Des*. **2008**, 8*,* 2824-2833. (h) Anantharaman, G.; Chandrasekhar, V.; Walawalkar, M. G.; Roesky, H. W.; Vidovic, D.; Magull, J.; Noltemeyer, M. Molecular zinc phosphonates: synthesis and X-ray crystal structures of [{$(ZnMe)_4(THF)_2$}{tBuPO_3}$_2$] and [{$(ZnEt)_3(Zn(THF))_3$}{tBuPO_3}$_4${μ_3-OEt}]. *Dalton Trans.* **2004**, 1271-1275. (i) Sahoo, D.; Suriyanarayanan, R.; Metre, R. K.; Chandrasekhar, V. Molecular and polymeric zinc(II) phosphonates: isolation of an octanuclear ellipsoidal ensemble. *Dalton Trans.* **2014**, *43*, 7304-7313.

7. (a) Coxall, R. A.; Harris, S. G.; Henderson, D. K.; Parsons, S.; Tasker, P. A.; Winpenny, R. E. P. Inter-ligand reactions: in situ formation of new polydentate ligands. *J. Chem. Soc., Dalton Trans.* **2000**, *0*, 2349-2356. (b) Zheng, Y.-Z.; Evangelisti, M.; Tuna, F.; Winpenny, R. E. P. Co–Ln Mixed-Metal Phosphonate Grids and Cages as Molecular Magnetic Refrigerants. *J. Am. Chem. Soc.***2012**, *134*, 1057-1065. (c) Harris, S. G. Crystallographic and modelling studies of organic ligands on metal surfaces. Ph.D. Thesis, The University of Edinburgh, 1999.

8. Chandrasekhar, V.; Kingsley, S.; Rhatigan, B.; Lam, M. K.; Rheingold, A. L. New Structural Forms in Molecular Metal Phosphonates: Novel Tri- and Hexanuclear Zinc(II) Cages Containing Phosphonate and Pyrazole Ligands. *Inorg. Chem.* **2002**, *41*, 1030-1032.

9. Chandrasekhar, V.; Sasikumar, P.; Boomishankar, R.; Anantharaman, G. Assembly of Lipophilic Tetranuclear (Cu_4 and Zn_4) Molecular Metallophosphonates from 2,4,6-Triisopropylphenylphosponic Acid and Pyrazole Ligands. *Inorg. Chem.* **2006**, *45*, 3344-3351.

10. Wu, J.; Song, Y.; Zhang, E.; Hou, H.; Fan, Y.; Zhu, Y. Studies on Cage-Type Tetranuclear Metal Clusters with Ferrocenylphosphonate Ligands. *Chem. Eur. J.* **2006**, *12*, 5823-5831.

11. (a) Murugavel, R.; Shanmugan, S. Seeking tetrameric transition metal phosphonate with a D4R core and organising it into a 3-D supramolecular assembly. *Chem. Commun.* **2007**, 1257-1259. (b) Murugavel, R.; Shanmugan, S. Assembling metal phosphonates in the presence of monodentate-terminal and bidentate-bridging pyridine ligands. Use of non-covalent and covalent-coordinate interactions to build polymeric metal–phosphonate architectures. *Dalton Trans.* **2008**, 5358-5367.

12. For representative examples of other metal phosphonates with D4R structures see (a) Chandrasekhar, V.; Nagarajan, L.; Cleérac, R.; Ghosh, S.; Verma, S. A Distorted Cubic Tetranuclear Copper(II) Phosphonate Cage with a Double-Four-Ring-Type Core. *Inorg. Chem.* **2008**, *47*, 1067-1073. (b) Baskar, V.; Shanmugam, M.; Sañudo, E. C.; Shanmugam, M.; Collison, D.; McInnes, E. J. L.; Wei, Q.; Winpenny, R. E. P. Metal cages using a bulky phosphonate as a ligand. *Chem. Commun.* **2007**, 37-39. (c) Walawalkar, M. G.; Horchler, S.; Dietrich, S.; Chakraborty, D.; Roesky, H. W.; Schäfer, M.; Schmidt, H.-G.; Sheldrick, G. M.; Murugavel, R. Novel Organic-Soluble Molecular Titanophosphonates with Cage Structures Comparable to Titanium-Containing Silicates. *Organometallics* **1998**, *17*, 2865-2868. (d) Chandrasekhar, V.; Dey, A.; Senapati, T.; Sañudo, E. C. Distorted cubic tetranuclear vanadium(IV) phosphonate cages: double-four-ring (D4R) containing transition metal ion phosphonate cages. *Dalton Trans.* **2012**, *41*, 799-803.

13. For Zn phosphates with D4R structures see (a) Murugavel, R.; Kuppuswamy, S.; Boomishankar, R.; Steiner, A. Hierarchical Structures Built from a Molecular Zinc Phosphate Core. *Angew. Chem. Int. Ed.* **2006**, *45*, 5536-5540. (b) Kalita, Alok Ch.; Gupta, Sandeep K.; Murugavel, Ramaswamy. A Solvent Switch for the Stabilization of Multiple Hemiacetals on an Inorganic Platform: Role of Supramolecular Interactions. *Chem. Eur. J.* **2016**, *22*, 6863-6875.

14. Crystallization of {Zn[**1**-H]}$_4$ from wet CH_3OH solution (ca. 0.03 M in Zn^{2+}) afforded crystals of {Zn[**1**-H](CH_3OH)$_{0.5}$}$_4$•{Zn[**1**-H](CH_3OH)$_{0.75}$}$_4$•6CH_3OH•2H_2O, which has the same core structure as {Zn[**1**-H](CH_3OH)}$_4$•12CH_3OH but features κ^1-bound sulfonate groups and two or four CH_3OH ligands per Zn_4 unit. See Supporting Information for details.

15. Fulmer, G. R.; Miller, A. J. M.; Sherden, N. H.; Gottlieb, H. E.; Nudelman, A.; Stoltz, B. M.; Bercaw, J. E.; Goldberg, K. I. NMR Chemical Shifts of Trace Impurities: Common Laboratory Solvents, Organics, and Gases in Deuterated Solvents Relevant to the Organometallic Chemist. *Organometallics* **2010**, *29*, 2176-2179.

16. Abdur-Rashid, K.; Fong, T. P.; Greaves, B.; Gusev, D. G.; Hinman, J. G.; Landau, S. E.; Lough, A. J.; Morris, R. H. An Acidity Scale for Phosphorus-Containing Compounds Including Metal Hydrides and Dihydrogen Complexes in THF: Toward the Unification of Acidity Scales. *J. Am. Chem. Soc.* **2000**, *122*, 9155-9171.

17. The P-O, Pd-O and Zn-O bond distances in **2** indicate that the positive charges are delocalized between Zn and Pd, but for simplicity the charges are placed on Zn in the drawing in Scheme 4.

18. A related dimeric Pd compound [{(κ^2-*P*,*SO*-**1**-Et_2)PdMe}$_2$(μ-Cl)]MgCl was shown to self-assemble around the Mg^{2+} cation. Contrella, N. D.; Jordan, R. F. Lewis Acid Modification and Ethylene Oligomerization Behavior of Palladium Catalysts That Contain a Phosphine-Sulfonate-Diethyl Phosphonate Ancillary Ligand. *Organometallics* **2014**, *33*, 7199-7208.

19. (a) Bukhaltsev, E.; Goldberg, I.; Cohen, R.; Vigalok, A. Tunable π-Interactions in Monomeric Organozinc Complexes: Solution and Solid-State Studies. *Organometallics* **2007**, *26*, 4015-4020. (b) Wooten, A.; Carroll, P. J.; Maestri, A. G.; Walsh, P. J. Unprecedented Alkene Complex of Zinc(II): Structures and Bonding of Divinylzinc Complexes. *J. Am. Chem. Soc.* **2006**, *128*, 4624-4631. (c) Lichtenberg, C.; Engel, J.; Spaniol, T. P.; Englert, U.; Raabe, G.; Okuda, J. Bis(allyl)zinc Revisited: Sigma versus Pi Bonding of Allyl Coordination. *J. Am. Chem. Soc.* **2012**, *134*, 9805-9811.

20. Zhou, X.; Lau, K.; Petro, B. J., Jordan, R. F. *cis/trans* Isomerization of *o*-Phosphino-Arenesulfonate Palladium Methyl Complexes. *Organometallics* **2014**, *33*, 7209-7214.

21. P-P coupling is normally observed when phosphine-phosphonate ligands chelate to Pd in a κ^2-*P*-P*O* coordination mode. (a) Johnson, A. M.; Contrella, N. D.; Sampson, J. R.; Zheng, M.; Jordan, R. F. Allosteric Effects in Ethylene Polymerization Catalysis. Enhancement of Performance of Phosphine-Phosphinate and Phosphine-Phosphonate Palladium Alkyl Catalysts by Remote Binding of $B(C_6F_5)_3$. *Organometallics* **2017**, *36*, 4990-5002. (b) Contrella, N. D.; Sampson, J. R.; Jordan, R. F. Copolymerization of Ethylene and Methyl Acrylate by Cationic Palladium Catalysts That Contain Phosphine-Diethyl Phosphonate Ancillary Ligands. *Organometallics* **2014**, *33*, 3546-3555. (c) Carrow, B. P.; Nozaki, K. Synthesis of Functional Polyolefins Using Cationic Bisphosphine Monoxide–Palladium Complexes. *J. Am. Chem. Soc.* **2012**, *134*, 8802-8805.

22. This mixture includes major species with low-field Pd-Me ^{1}H NMR resonances (δ 0.91, 0.80, ca. 80 %) suggestive of mononuclear structures. A species tentatively identified as the 4-^{t}Bu-py analogue of **3**-py on the basis of its high-field Pd-Me ^{1}H NMR resonance (δ -0.83) is also formed in low yield (ca. 10 %).

23. Addition of CD_3OD to a solution of **3-py** in CD_2Cl_2 also sharpens the NMR spectra.

24. Some formation of **3**-py was observed during attempts to recrystallize **4**-py from CH_2Cl_2/Et_2O and toluene/Et_2O, suggesting that Et_2O also induces this conversion.

25. Kyba, E. P. Nucleophilic substitution at phosphorus in tertiary phosphines. Evidence against pseudorotation in a potential intermediate. *J. Am. Chem. Soc.* **1976**, *98*, 4805-4809.

26. Bonnaventure, I.; Charette, A. B. Probing the Importance of the Hemilabile Site of Bis(phosphine) Monoxide Ligands in the Copper-Catalyzed Addition of Diethylzinc to N-Phosphinoylimines: Discovery of New Effective Chiral Ligands. *J. Org. Chem.* **2008**, *73*, 6330-6340.

27. De Graaf, W.; Boersma, J.; Smeets, W. J. J.; Spek, A. L.; Van Koten, G. Dimethyl(N,N,N',N'-tetramethylethanediamine)palladium(II) and dimethyl[1,2-bis(dimethylphosphino)ethane]palladium(II): syntheses, x-ray crystal structures, and thermolysis, oxidative-addition and ligand-exchange reactions. *Organometallics* **1989**, *8*, 2907-2917.

28. (a) Calvin, G.; Coates, G. E. Organopalladium compounds. *J. Chem. Soc.* **1960**, 2008-2016. (b) Foley, S. R.; Stockland, R. A.; Shen, H.; Jordan, R. F. Reaction of Vinyl Chloride with Late Transition Metal Olefin Polymerization Catalysts. *J. Am. Chem. Soc.* **2003**, *125*, 4350-4361. (c) Lau, K.-C.; Petro, B. J.; Bontemps, S.; Jordan, R. F. Comparative Reactivity of Zr– and Pd–Alkyl Complexes with Carbon Dioxide. *Organometallics* **2013**, *32*, 6895-6898.

29. Grinshpun, V.; Rudin, A. Measurement of Mark-Houwink constants by size exclusion chromatography with a low angle laser light scattering detector. *Makromol. Chem., Rapid Commun.* **1985**, 6, 219-223.

TOC graphic